International Journal of GEOMATE, April, 2018 Vol. 14, Issue 44, pp. 1-7
Geotec., Const. Mat. & Env., DOI: https://doi.org/10.21660/2018.44.7285
ISSN: 2186-2982 (Print), 2186-2990 (Online), Japan

ANALYSIS OF AXIAL LOADED PILE IN MULTILAYERED SOIL USING NODAL EXACT FINITE ELEMENT MODEL

*Chinnapat Buachart[1], Chayanon Hansapinyo[2] and Worsak Kanok-Nukulchai[3]

[1, 2] Center of Excellence for Natural Disaster Management, Department of Civil Engineering, Faculty of Engineering, Chiang Mai University, Thailand;

[3] Asian Institute of Technology, Thailand

*Corresponding Author, Received: 19 June 2017, Revised: 29 Nov. 2017, Accepted: 30 Dec. 2017

ABSTRACT: The nodal exact displacement based finite element method for analyzing axially loaded pile embedded in multilayered of finite depth of elastic soil is presented. The condition of shape function by which exact value may be reproduced at the nodal points regarding a few number of elements is investigated. The examined shape functions which satisfy the homogeneous governing equations in each layer of elastic soil are introduced to obtain the so-called exact element stiffness matrix. Then the stiffness matrix of proposed shape function was constructed via total potential energy principle. The results obtained from proposed finite element were compared with analytical solutions from literature. Axial force and displacement solutions of the pile embedded in multilayered soil obtained from proposed finite element model show exact agreement with analytical solutions and data from the available literature.

Keywords: Axially loaded pile, Displacement method, Finite element, Multilayer soil

1. INTRODUCTION

In this study, the displacement of axially loaded pile embedded in multi-layer soil is solved via proposed finite element procedure. The nodal exact shape function concept suggested in [1]–[4] are used to construct the stiffness matrix and equivalent nodal force incorporate with fixed-point iteration algorithm to solve nonlinear algebraic equations. In each iteration step, the coefficients of differential equation describe pile settlement behavior were estimated easily via the component of stiffness matrix and nodal displacement obtained from previous iteration step.

Examples of elastostatic pile embedded in multilayered soil subjected to quasi-static point load on topsoil level were analyzed [5]. The results from proposed element are compared with analytical solutions obtained from [6] to verify the accuracy of proposed pile element.

2. MATHEMATICAL FORMULATION

In this section, the governing equation of axisymmetric problem will be derived. Then the finite element formulation and solution scheme to obtain the nodal displacement will be described.

2.1 Problem Definition

The analysis considers a single circular cross-section pile [5], with radius r_p and total length L_p embedded in a total of N horizontal soil layer (Fig. 1). The pile is subjected to an axial force Q_t at the pile head which is flush with the ground surface. The pile itself crosses m layers ($m < N$). All soil layers are assumed to extend to infinity in the radial direction, and the bottom layer (N^{th} layer) also extends to infinity in downwards direction (half-space) as shown in Fig. 1. The soil medium in any layer (i^{th} layer, where $i = 1,\ldots, N$) is assumed to be elastic and isotropic material, with elastic properties described by soil shear modulus G_{si} and Poisson's ratio ν_{si}. The vertical depth from the ground surface to the bottom of any layer i is denoted by H_i. Hence, the thickness of each layer L_i is computed by the difference of bottom depth $H_i - H_{i-1}$ with $H_0 = 0$. The pile is assumed to behave as an elastic column with Young's modulus E_p. The Poisson's ratio of the pile material is neglected.

2.2 Governing Differential Equations

Since the cylindrical pile settlement problem in Fig. 1 is axisymmetric. Hence, we use the system of cylindrical coordinates (r-z coordinate) to indicate any position in pile and soil bodies. The origin of cylindrical coordinate coincides with the center of pile cross section at the pile head level. The vertical (positive in the downward direction) coordinate z-axis coincides with pile axis. The non-slip conditions between pile surface and surrounding soil and between soil layers are assumed. The vertical displacement $u_z(r,z)$ at any point in the soil is represented as the product of two functions in r and z coordinates as follows:

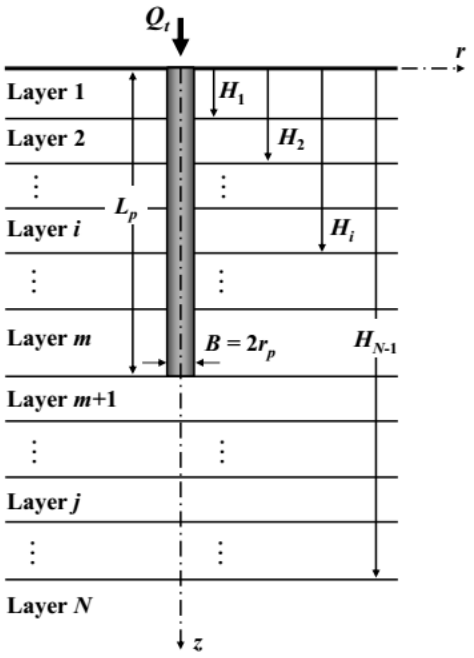

Fig. 1 Axially loaded pile and multi-layer soil, modified from [5]

$$u_z(r,z) = w(z)\cdot\phi(r) \tag{1}$$

where $w(z)$ is the vertical displacement of the pile at any point along pile axis, and $\phi(r)$ is the soil displacement decay function in the radial direction.

To compute the strain and stress in the elastic soil medium, the displacement in the radial component is assumed to be small compared with vertical displacement in Eq. (1), *i.e.* $u_r = 0$. Hence, the nonzero strain components in elastic soil medium can be expressed as:

$$\begin{bmatrix}\varepsilon_{zz}\\ \gamma_{rz}\end{bmatrix} = \begin{bmatrix}\dfrac{\partial u_z}{\partial z}\\ \dfrac{\partial u_z}{\partial r}+\dfrac{\partial u_r}{\partial z}\end{bmatrix} = \begin{bmatrix}\phi(r)\dfrac{\partial w(z)}{\partial z}\\ w(z)\dfrac{\partial \phi(r)}{\partial r}\end{bmatrix} \tag{2}$$

and stress in soil medium can be computed following the Hooke's Law:

$$\begin{bmatrix}\sigma_{rr}\\ \sigma_{\theta\theta}\\ \sigma_{zz}\\ \sigma_{rz}\end{bmatrix} = \begin{bmatrix}\lambda_s & 0\\ \lambda_s & 0\\ \lambda_s+2G_s & 0\\ 0 & G_s\end{bmatrix}\begin{bmatrix}\varepsilon_{zz}\\ \gamma_{rz}\end{bmatrix} \tag{3}$$

where λ_s and G_s are the elastic constants of soil.

Then, the calculus of variations is used to obtain the governing differential equation in a pile and surrounding soil by defining the strains from displacement functions in Eq. (1), and prescribe the variation of total potential energy with respect to w and ϕ equal to zeros [6]. The governing differential equation due to variation with respect to w for the pile and soil below the pile tip is as follow:

$$-\left(E_iA_i+2t_i\right)\frac{d^2w_i}{\partial z^2}+k_{si}w_i = 0 \tag{4}$$

where $E_i = E_p$ and $A_i = A_p$ when $1 \le i \le m$ (along pile axis), and $E_i = \lambda_{si} + 2G_{si}$ and $A_i = \pi r_p^2$ when $(m + 1) \le i < N$ (soil below the pile tip). The elastic constant $\lambda_{si} + 2G_{si}$ is a function of Poisson's ratio ν_{si} and shear modulus G_{si} of soil:

$$\lambda_{si}+2G_{si} = \frac{2G_{si}\left(1-\nu_{si}\right)}{\left(1-2\nu_{si}\right)} \tag{5}$$

Note that the coefficients k_{si}, and t_i represent the shear and compressive resistances of soil mass against pile settlement. Both k_{si}, and t_i are a function of decay function ϕ and elastic properties of soil as follow:

$$k_{si} = 2\pi G_{si}\int_{r_p}^{\infty} r\left(\frac{d\phi}{dr}\right)^2 dr \tag{6}$$

$$t_i = \pi(\lambda_{si}+2G_{si})\int_{r_p}^{\infty} r\phi^2 dr \tag{7}$$

The governing differential equation for the soil surrounding the pile can be obtained by taking the variation of total potential energy with respect to ϕ equals to zero:

$$\frac{d^2\phi}{dr^2}+\frac{1}{r}\frac{d\phi}{dr}-\left(\frac{\gamma_r}{r_p}\right)^2\phi = 0 \tag{8}$$

where

$$\frac{\gamma_r}{r_p} = \sqrt{\frac{n_s}{m_s}} \tag{9}$$

$$m_s = \sum_{i=1}^{N} G_{si}\int_{H_{i-1}}^{H_i} w_i^2 dz \tag{10}$$

$$n_s = \sum_{i=1}^{N}(\lambda_{si}+2G_{si})\int_{H_{i-1}}^{H_i}\left(\frac{dw_i}{dz}\right)^2 dz \tag{11}$$

and the solution of Eq. (8) with boundary conditions $\phi(r) = 0$ at r extend to infinity, and $\phi(r) = 1$ at $r = r_p$ is a zero order modified Bessel function of the second kind:

$$\phi(r) = \frac{K_0\left(\frac{\gamma_r}{r_p} r\right)}{K_0\left(\gamma_r\right)}; \; r_p \le r \le \infty \tag{12}$$

Substituting decay function $\phi(r)$ into Eqs. (6) and (7), obtain the explicit formula for coefficients k_{si} and t_i in terms of modified Bessel function of the second kind, zero and first orders [6]:

$$k_{si} = \pi G_{si}\left[\gamma_r^2\left(1-\eta^2\right)+2\gamma_r\eta\right] \tag{13}$$

$$t_i = \frac{1}{2}\pi r_p^2\left(\lambda_{si}+2G_{si}\right)\left(\eta^2-1\right) \tag{14}$$

where the coefficient η is the ratio between the modified Bessel function of the second kind of the first-order K_1 and zero order K_0, *i.e.*:

$$\eta = \frac{K_1\left(\gamma_r\right)}{K_0\left(\gamma_r\right)} \tag{15}$$

The general solution of Eq. (4) is given by:

$$w_i\left(z\right) = B_i\cosh\left(\alpha_i z\right)+C_i\sinh\left(\alpha_i z\right) \tag{16}$$

where B_i and C_i are integration constant. The characteristic parameter α_i of pile and soil interaction is expressed as follow:

$$\alpha_i = \sqrt{\frac{k_{si}}{\left(E_iA_i+2t_i\right)}} \tag{17}$$

Note that the dimension of parameter α_i is an inversion of length. An axial force $Q_i(z)$ at a depth z in the i^{th} layer is obtained defined as:

$$Q_i\left(z\right) = -\left(E_iA_i+2t_i\right)\frac{dw_i}{dz} \tag{18}$$

or explicitly in the form:

$$Q_i\left(z\right) = -a_i\left[B_i\sinh\left(\alpha_i z\right)+C_i\cosh\left(\alpha_i z\right)\right] \tag{19}$$

where $a_i = \alpha_i\left(E_iA_i + 2t_i\right)$, the integration constants B_i and C_i in Eqs. (16) and (19) can be determined analytically from the procedure proposed in [5].

2.3 Finite Element Formulation

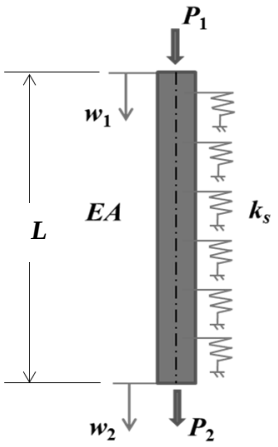

Fig. 2 Axially loaded pile element and element degrees of freedom, modified from [4]

In the previous works [5, 6]; integration constants B_i and C_i for all layers were solved by applying directly the boundary conditions for the pile load head, bottom end, and layer interfaces to the algebraic system of equations. Then the authors simplified the calculation by the determinant of the matrix of the algebraic system.

The equation at all soil interfaces can also be constructed automatically through the assembly of finite element stiffness. The boundary conditions at all soil interfaces need not be constructed separately. Hence, in this section, the formula of stiffness matrix via total potential energy and exact interpolation function will be described and will be used to test with analytical problems from literature.

Consider one-dimensional element in Fig. 2, which represents the portion of pile embedded in any one layer of surrounding soil governed by Eq. (4). Assuming that soil surrounding pile element is in an elastic condition for the whole length. Shear resistance of soil is represented by equivalent soil spring coefficient k_{si}. Pile element in Fig. 2 composes of two nodes at top and bottom, numbering with node 1 and 2, respectively. The total potential energy of this soil-pile element subjected to an equivalent nodal forces P_1 and P_2 is defined as the sum of internal potential energy (strain energy) and the external potential energy due to external load as follow [4]:

$$\Pi = \frac{1}{2}\left[\left(E_i A_i + 2t_i\right)\int_0^L \left(\frac{dw}{dz}\right)^2 dz + k_{si}\int_0^L w^2 dz \right] - P_1 w_1 - P_2 w_2 \quad (20)$$

where $w(z)$ is the vertical pile displacement at depth z where $0 \le z \le L$. The first variation of Eq. (20) leads to:

$$\delta\Pi = \left(E_i A_i + 2t_i\right)\int_0^L \left(\frac{d\delta w}{dz}\right)\left(\frac{dw}{dz}\right)dz + k_{si}\int_0^L \left(\delta w\right) w dz - P_1\delta w_1 - P_2\delta w_2 \quad (21)$$

Note that the origin of vertical coordinate along the pile axis in potential function, Eq. (20), is now moved to the top node of pile portion, instead of pile head on ground level. The nodal displacement at the top and bottom nodes are denoted by w_1 and w_2, respectively. Suppose that the pile portion at the i^{th} layer is considered, the pile length can be computed from different of bottom depth between nearby soil layer, *i.e.* $L = H_i - H_{i-1}$.

Applying the appropriate Gauss-Green theorem to Eq. (21) and setting $\delta\Pi = 0$, gives the differential equation for equilibrium similar to Eq. (4), and a set of natural boundary conditions as follows

$$P_1 = -\left(E_i A_i + 2t_i\right)\left.\frac{dw}{dz}\right|_{z=0} \quad (22)$$

$$P_2 = \left(E_i A_i + 2t_i\right)\left.\frac{dw}{dz}\right|_{z=L} \quad (23)$$

The natural boundary condition at first node, Eq. (22) is similar to axial load expression in Eq. (18).

2.4 Exact Interpolation Function

To construct the system of algebraic equations with respect to nodal displacement, the trial solution of $w(z)$ in Fig. 2 is introduced in the form:

$$w(z) = N_1(z)w_1 + N_2(z)w_2 \quad (24)$$

The shape functions in Eq. (24) are taken from a homogeneous solution of Eq. (4), *i.e.*

$$N_1(z) = \frac{\sinh\left[\alpha_i\left(L - z\right)\right]}{\sinh\beta_i} \quad (25)$$

$$N_2(z) = \frac{\sinh\left(\alpha_i z\right)}{\sinh\beta_i} \quad (26)$$

where the dimensionless parameter $\beta_i = \alpha_i L$.

In present work, the proposed finite element procedure to solve Eq. (4) for a given load Q_t (Fig. 1) will be explained in next section. Then, the results from proposed nodal exact element will be compared with an available analytical solution in [5, 6].

2.5 Iteration Scheme

According to Eqs. (10) and (11), the shape parameter of decay function, namely γ_r in Eqs. (8) and (9) depends on pile settlement $w(z)$. Hence, the finite element discretization of Eq. (21) with trial displacement function in Eq. (24) leads to the steady steady-state set of non-linear algebraic equations as follow:

$$\mathbf{K}(\mathbf{w})\mathbf{w} = \mathbf{f} \quad (27)$$

In which stiffness matrix **K** is a non-linear function of nodal displacement **w**. The external nodal load **f** is presented in term of specified vector. To solve the nodal solution from Eq. (27), we employed the fixed point iteration technique as follows [7]:

$$\mathbf{K}^{(n-1)}\mathbf{w}^{(n)} = \mathbf{f} \quad (28)$$

where $\mathbf{K}^{(n-1)} = \mathbf{K}(\mathbf{w}^{(n-1)})$, $n = 1,2,\ldots$; is stiffness matrix evaluated from nodal solution **w** at previous iteration step. Usually, iteration process in Eq. (28) is repeated until the value of nodal solution **w** converged. In this work, we will use convergence criteria of the parameter γ_r instead. Hence, the convergence criteria for all cases are:

$$\left|\gamma_r^{(n)} - \gamma_r^{(n-1)}\right| < 10^{-5} \quad (29)$$

Note that the convergence criteria used in Eq. (29) is similar to criteria used in [5, 6] and also results in the convergence of nodal solution **w** in Eq. (27).

2.6 Derivation of Element Stiffness Matrix

Refer to the first variation of strain energy terms in Eq. (21), the element stiffness matrix for pile and soil can be expressed as follows:

$$K_{ab}^{pile} = \left(E_i A_i + 2t_i\right)\int_0^L \left(\frac{dN_a}{dz}\right)\left(\frac{dN_b}{dz}\right)dz \qquad (30)$$

$$K_{ab}^{soil} = k_{si}\int_0^L N_a N_b dz \qquad (31)$$

where the indices *a* and *b* represent element nodal number, ranged from 1 to 2.

2.6.1 Element stiffness matrix

Substituting shape functions from Eq. (25) and (26) into element stiffness formulation in Eq. (30) and (31), the component of element stiffness matrices can be explicitly expressed as

$$\begin{aligned} K_{11}^{pile} &= K_{22}^{pile} = \frac{a_i}{2}\left(\beta_i \mathrm{csch}^2\beta_i + \coth\beta_i\right) \\ K_{12}^{pile} &= K_{21}^{pile} = -\frac{a_i}{2}\,\mathrm{csch}\,\beta_i\left(1+\beta_i\coth\beta_i\right) \end{aligned} \qquad (32)$$

and

$$\begin{aligned} K_{11}^{soil} &= K_{22}^{soil} = \frac{k_{si}}{2\alpha_i}\left(\coth\beta_i - \beta_i\mathrm{csch}^2\beta_i\right) \\ K_{12}^{soil} &= K_{21}^{soil} = -\frac{k_{si}}{2\alpha_i}\,\mathrm{csch}\,\beta_i\left(1-\beta_i\coth\beta_i\right) \end{aligned} \qquad (33)$$

Hence, the total stiffness matrix of layer *i*, which is the summation of stiffness in Eqs. (32) and (33), can be defined as:

$$\mathbf{K}_i = a_i\begin{bmatrix} \coth\beta_i & -\mathrm{csch}\beta_i \\ -\mathrm{csch}\beta_i & \coth\beta_i \end{bmatrix} \qquad (34)$$

where parameter a_i was already defined in Eq. (19). The element stiffness matrices in Eq. (34) are assembled to form global stiffness in Eq. (27).

2.6.2 Stiffness of bottom-most layer

At the bottom-most layer (layer *N*), the thickness is assumed to be infinity, and nodal displacement at the bottom most point is prescribed to zero. Hence, the element stiffness matrix in Eq. (34) has to be redefined. Convergence of hyperbolic function when $L\to\infty$ shows that the element stiffness matrix for N^{th} layer is similar to penalty spring coefficient [8] attached to N^{th} degree of freedom, w_N, with the following form:

$$k_{NN} = a_N = \alpha_N\left(E_N A_N + 2t_N\right) \qquad (35)$$

The convergence of hyperbolic function also shows that the displacement in the N^{th} layer can be interpolated via the form below:

$$w(z) = w_N\left[\cosh\left(\alpha_N z\right) - \sinh\left(\alpha_N z\right)\right] \qquad (36)$$

The interpolation of *w* in Eqs. (24) and (36) are then used to compute axial force according to Eq. (18). Note that coordinate *z* in Eqs. (24)–(36) is local coordinate defined in i^{th}-layer.

2.6.3 Calculation of decay parameter

The value of decay parameter γ_r in any iteration step of Eq. (28) can be evaluated from nodal displacement solution **w** in each step. Substituting the displacement function, Eq. (24), into Eqs. (10) and (11) obtained:

$$\begin{aligned} m_s = \sum_{i=1}^{N-1}\frac{G_{si}}{2\alpha_i}&\begin{bmatrix} \left(\coth\beta_i - \beta_i\mathrm{csch}^2\beta_i\right)\left(w_i^2 + w_{i+1}^2\right) - \\ 2w_i w_{i+1}\,\mathrm{csch}\,\beta_i\left(1-\beta_i\coth\beta_i\right) \end{bmatrix} \\ &+ \frac{G_{sN}}{2\alpha_N}w_N^2 \end{aligned} \qquad (37)$$

$$\begin{aligned} n_s = \sum_{i=1}^{N-1}\frac{\alpha_i\bar{E}_{si}}{2}&\begin{bmatrix} \left(\beta_i\mathrm{csch}^2\beta_i + \coth\beta_i\right)\left(w_i^2 + w_{i+1}^2\right) - \\ 2w_i w_{i+1}\,\mathrm{csch}\,\beta_i\left(1+\beta_i\coth\beta_i\right) \end{bmatrix} \\ &+ \frac{\alpha_N\bar{E}_{sN}}{2}w_N^2 \end{aligned} \qquad (38)$$

where $\bar{E}_{si} = \lambda_{si} + 2G_{si}$; the values m_s and n_s are then substituted in Eq. (9) to compute the value of the parameter γ_r.

3. NUMERICAL EXAMPLES

In this section, two numerical examples are presented to illustrate the effectiveness of nodal exact finite element proposed in the previous section. Results from proposed element are verified using analytical solutions available in [5, 6].

3.1 Pile with Ideal Rigid End Bearing

In this example, we study the behavior of pile in homogeneous soil (one layer) subjected to pile head load as shown in Fig. 3. The ratio of pile elastic modulus and soil shear modulus is set to be E_p/G_s = 3000, and Poisson's ratio ν_s = 0.4999. The pile tip is assumed to rest on a rigid layer and pile diameter $B = 2r_p$ = 0.2 m. Note that this problem was already solved in [6], and repeat here to verify our proposed finite element model. Because the value of Poisson's ratio is close to 0.5, the modulus λ_s is approach infinity, according to Eq. (5). Hence, this problem will set the value of modulus λ_s equals to

zero and replace the value of G_s by equivalent soil shear modulus [5]:

$$G_s^* = 0.75G_s\left(1+0.25v_s^2\right) \quad (39)$$

Figure 4 shows the relation between the normalized pile head stiffness K_N versus normalized pile length L_p/B. The normalized pile head stiffness is defined as the ratio of load at pile head versus settlement at pile head normalized by E_pB, *i.e.* $K_N = Q_t/(w_0E_pB)$ where w_0 = settlement at pile head. The plot in Fig. 4 was obtained with the finite element analysis proposed in this work and from the analytical method in the previous study [5]. The normalized pile head stiffness in Fig. 4 decreases with increasing of normalized pile length. The results of finite element analysis presented in this work are in good agreement with the previous study in [6].

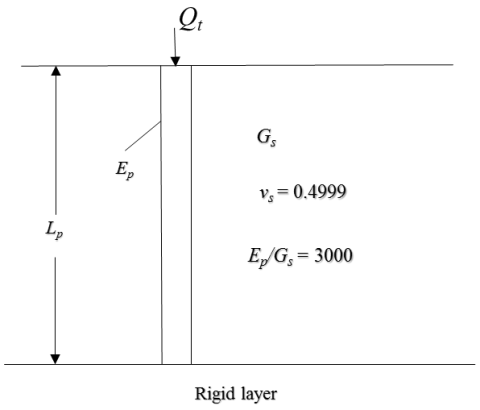

Fig. 3 Pile rest on rigid layer, modified from [6]

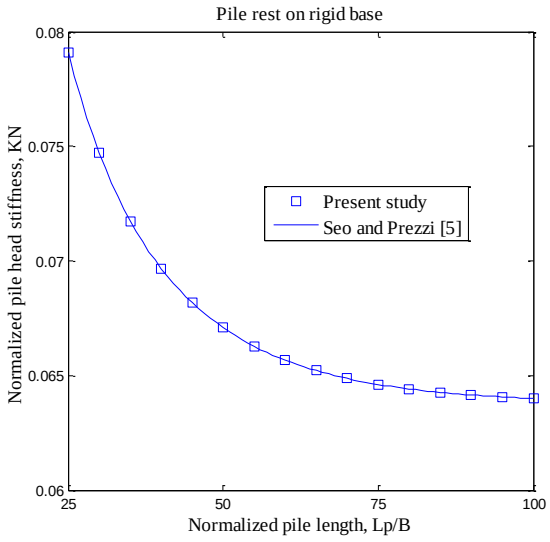

Fig. 4 Normalized pile head stiffness versus normalized pile length of rigid-end pile

3.2 Micropile (Italy)

This example presents the case of micro-pile, which was installed in a complex soil profile [6]. The soil profile and pile length are shown in Fig. 5. Pile diameter and length are equal to 0.2 m and 19 m, respectively. Modulus of elasticity of pile is approximately 27 GPa. In all soil layers, the Poisson's ratio was assumed to be 0.3. The values of soil depth, shear modulus, and Poisson's ratio of Fig. 5 are listed in Table 1. The numerical test was performed using four proposed nodal exact elements with four active degrees of freedom. The value of stiffness for bottom most soil was calculated according to Eq. (35).

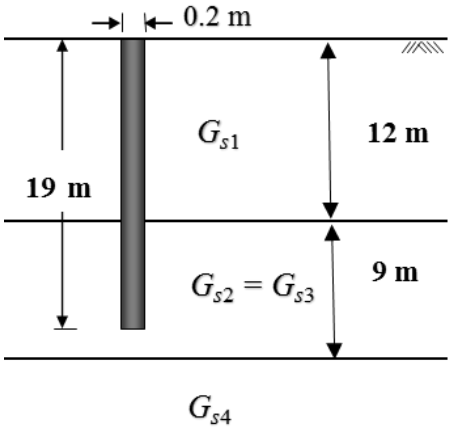

Fig. 5 Soil Profile of Italy case, modified from [5]

Table 1 Input properties for the analysis of micropile tested in Italy (B = 0.2 m, L_p = 19 m, E_p = 27 GPa)

Layer	H_i (m)	G_{si} (MPa)	v_{si}
1	12	19.2	0.3
2	19	45.0	0.3
3	21	45.0	0.3
4	∞	53.1	0.3

Figure 6 shows the calculated pile head settlement versus input pile head load. Figure 7 shows measured and calculated load-transfer curves for applied load equal to 50, 250, and 500 kN. These figures show that there is very good agreement between the proposed finite element and analytical solution in the literature [5].

4. CONCLUSION

The finite element model for pile embedded in multilayered elastic soil subjected to axial load is proposed. The system of nonlinear algebraic

equations constructed from proposed finite element has been solved via fixed point iteration technique. The values of the nodal solution are recalculated until the shape parameter of decay function converged.

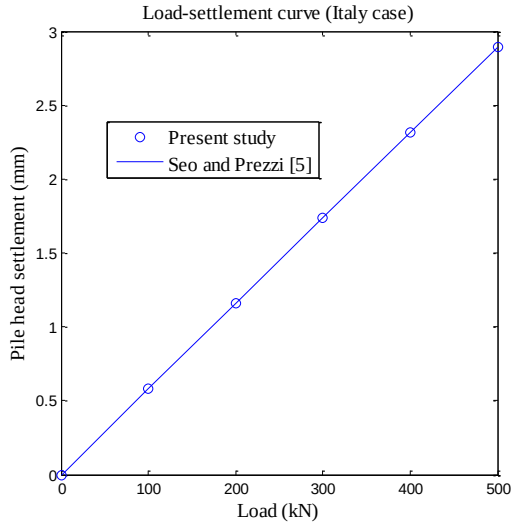

Fig. 6 Load-settlement curve at pile head (Italy case)

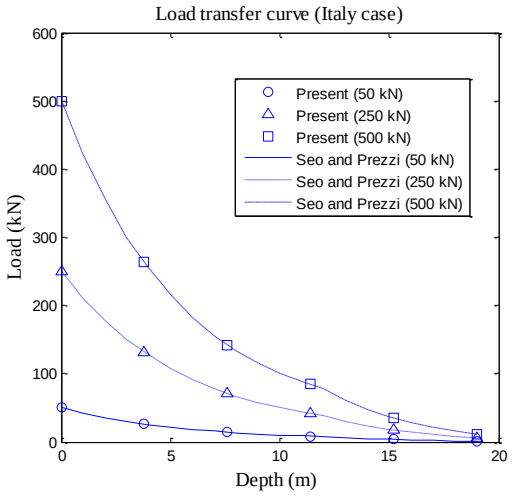

Fig. 7 Load-transfer curve for pile head load equal to 50, 250, and 500 kN (Italy case)

Numerical examples for static load pile embedded in multilayered elastic soil were tested by proposed finite element compare with available analytical solutions from literature.

Two problems, composed of pile resting on the rigid base, and pile embedded in four layers soil with infinite bottom depth were solved to obtain pile settlement and load transfer curves. The numerical test indicates that the proposed finite element method are very good agreement with the available analytical solution proposed in the literature.

5. ACKNOWLEDGEMENTS

The author gratefully acknowledges the financial support received from Thailand Research Fund (New Researcher Grant TRG5880066).

6. REFERENCES

[1] Tong P, "Exact solutions of certain problems by finite element method", AIAA J., Vol. 7, 1969, pp. 178-180.

[2] Kanok-Nukulchai W, Dayawansa PH, and Karasudhi P, "An exact finite element model for deep beams", Int. J. of Struc, Vol. 1, Jan. 1981, pp. 1-7.

[3] Ma H, "Exact solutions of axial vibration problems of elastic bars", Int. J. Numer. Meth. Eng., Vol. 75, 2008, pp. 241-252.

[4] Buachart C, Hansapinyo C, and Sommanawat W, "An exact displacement based finite element model for axially loaded pile", Int. J. of GEOMATE, Sept., Vol. 11(25), 2016, pp. 2474-2479.

[5] Seo, H and Prezzi, M, "Analytical solutions for a vertically loaded pile in multilayered soil", Geomechanics and Geoengineering: An International Journal, Vol. 2(1), 2007, pp. 51–60.

[6] Seo, H, Prezzi, M, and Salgado, R, "Settlement analysis of axially loaded pile", International Conference on Case Histories in Geotechnical Engineering, Vol. 27, 2008, pp. 1–8.

[7] Chapra SC, Applied Numerical Methods with Matlab for Engineers and Scientists. McGraw-Hill, 2005.

[8] Zienkiewicz OC and Taylor RL, The Finite Element Method. Vol. I. Oxford: Butterworth-Heinemann, 2000.